Journal of Robotics and Control (JRC)
Volume 6, Issue 5, 2025
ISSN: 2715-5072, DOI: 10.18196/jrc.v6i5.26609

An Explainable CNN–LSTM Framework for Monthly Crude Oil Price Forecasting Using WTI Time Series Data

Joompol Thongjamroon [1], Songgrod Phimphisan [2], Nattavut Sriwiboon [3*]
[1] Department of Business Computer, Faculty of Administrative Science, Kalasin University, Kalasin, Thailand
[2, 3] Department of Computer Science and Information Technology, Faculty of Science and Health Technology, Kalasin University, Kalasin, Thailand
Email: [1] joompol.th@ksu.ac.th, [2] songgrod.ph@ksu.ac.th, [3] nattavut.sr@ksu.ac.th
*Corresponding Author

***Abstract*—Crude oil price forecasting has posed significant challenges due to its volatility and nonlinear dynamics. This study has proposed an explainable CNN–LSTM framework to predict monthly West Texas Intermediate (WTI) crude oil prices. The model has captured both local and sequential patterns without using external inputs or decomposition. Trained over 50 epochs across three data splits, it has been evaluated using RMSE, MAE, MASE, SMAPE, and directional accuracy. A classification accuracy of 92.4% and directional accuracy of up to 87.4% have been achieved. The model has consistently outperformed classical and hybrid baselines, with statistical significance confirmed by the Friedman–Nemenyi test. Saliency-based interpretability has further enhanced transparency, making the framework suitable for real-world energy forecasting.**

Keywords—Crude Oil Price Forecasting; CNN–LSTM Hybrid Model; Time Series Prediction; WTI; Deep Learning.

I. INTRODUCTION

Crude oil has played a pivotal role in shaping global economic stability, energy policy, and financial markets. Among various petroleum benchmarks, West Texas Intermediate (WTI) [1], [2] crude oil has been widely recognized as a standard reference in international oil pricing. However, forecasting crude oil prices has remained a complex task due to the influence of geopolitical events, supply–demand imbalances, macroeconomic fluctuations, and nonlinear market behavior. Accurate and timely forecasting models are therefore essential for risk management, investment strategies, and policy-making within the energy sector.

Traditional statistical models such as autoregressive integrated moving average (ARIMA) [3], generalized autoregressive conditional heteroskedasticity (GARCH) [1], and exponential smoothing have been extensively used for oil price forecasting. While these models have offered interpretability and ease of implementation, their performance has been limited by strong linearity assumptions and weak adaptability to non-stationary patterns in crude oil time series. To overcome these limitations, machine learning (ML) [4] models, including support vector regression (SVR), decision trees, and ensemble methods, have been introduced to handle nonlinearity [5]-[9]. Despite improved performance, most ML models have lacked the ability to retain long-term temporal dependencies critical in time series prediction. Recent advances in deep learning (DL) [10] have introduced powerful neural network architectures capable of learning complex [11]-[22] representations from raw sequences [23]-[27]. Models such as convolutional neural networks (CNNs) [28], long short-term memory (LSTM) [29] networks, and attention-based transformers have demonstrated substantial progress [17], [30]-[37] in financial forecasting, energy demand modeling, and economic prediction [38]-[43]. Hybrid DL models, in particular, have gained attention for combining complementary architectures such as CNN [31], [44]-[60] for local pattern recognition and LSTM for sequence modeling. Nevertheless, many existing studies have depended on signal decomposition techniques or external variables, which may increase computational cost and reduce generalizability.

To address these [61]-[69] gaps, an explainable CNN–LSTM framework has been proposed in this study for monthly WTI crude oil price forecasting. The model has been designed to operate end-to-end without requiring decomposition or external data, while capturing both short- and long-term dynamics in the input series. Saliency-based gradient analysis has been integrated to enhance interpretability, allowing users to understand which historical points have influenced the model's forecasts. A comprehensive evaluation has been conducted using the WTI dataset from 1986 to 2022, demonstrating the model's superiority over classical, ML-based, and decomposition-enhanced forecasting methods. The contributions of this paper can be summarized as follows:

- An end-to-end CNN–LSTM hybrid model has been developed for monthly crude oil forecasting using only historical price data.
- Model interpretability has been introduced through gradient-based saliency mapping to highlight influential time steps.
- The model has been evaluated using multiple error and directional metrics across varying train splits.
- Comparative analysis with nine related works has been provided, demonstrating consistent improvements in accuracy, efficiency, and transparency.

II. RELATED WORK

Numerous studies have been conducted using monthly WTI crude oil prices to forecast trends, understand volatility, and develop reliable prediction models. These efforts have spanned across statistical, ML, and DL domains. However, limited focus has been placed on incorporating explainable and transformer-based architectures into such forecasting tasks.

The previous study by Zhang *et al.* [61] has proposed a hybrid approach by integrating least squares support vector machines (LSSVM) [70] with particle swarm optimization (PSO) [71]-[81] for forecasting WTI crude oil prices from 1986 onward. Enhanced performance has been achieved through optimized hyperparameter tuning, although explainability and sequential learning have not been addressed. Chen *et al.* [62] have investigated a hybridization of the random walk model with ARMA using WTI data from the 1990s. While improvements in prediction accuracy have been demonstrated through statistical combinations, limitations related to nonlinearity and dynamic temporal dependencies have remained unresolved. Safari and Davallou [63] have applied hybrid state-space modeling in combination with ARIMA for monthly WTI forecasting. Their model has shown strength in capturing structural components, but it has not incorporated advanced nonlinear learning techniques or deep architectures. Pang *et al.* [64] have introduced a wavelet neural network (WNN) trained on monthly WTI data beginning in 1994. This approach has aimed to capture both time-frequency patterns and nonlinearities, although modern attention-based networks have not been explored. Kumar *et al.* [65] have developed a hybrid model combining variational mode decomposition (VMD) with LSTM using data from 2000 onwards. The VMD technique has been used to extract signal components, which have been modeled independently using deep sequence learners, resulting in improved predictive accuracy. Mohsin and Jamaani [66] have constructed a CNN-based model using monthly WTI data, targeting the forecasting of price volatility rather than trend direction. Although their results have demonstrated effectiveness, neither mode decomposition nor interpretability mechanisms have been incorporated. Khullar *et al.* [67] have proposed a Bi-LSTM model for monthly WTI prediction beginning in the 2010s. Bidirectional temporal learning has been applied to model historical dependencies, but the absence of hybridization or model explanation has limited practical interpretability. Qin *et al.* [68] have introduced an ensemble learning framework for WTI forecasting using Google Trends data as an external feature. Although various ML models have been combined, transparency in feature influence and decomposition strategies have not been emphasized. Purohit and Panigrahi [69] has provided one of the most comprehensive comparisons by employing four decomposition techniques (CEEMDAN, VMD, EMD, EEMD) in conjunction with 27 forecasting models on WTI data spanning from 1986 to 2022. Despite achieving notable accuracy with VMD-Huber Regression, model explainability and transformer-based learning have not been investigated.

In light of these gaps, an explainable forecasting model based on transformer architecture has been proposed in this paper. This model has been developed to surpass the performance of traditional hybrid and decomposition-based models while introducing enhanced interpretability and computational efficiency using the same monthly WTI crude oil dataset.

III. PROPOSED METHODOLOGY

To overcome the limitations of previous hybrid models and enhance forecasting accuracy while capturing both local and sequential dependencies, a DL framework based on a CNN–LSTM hybrid architecture has been developed. The methodology has been structured to extract temporal features hierarchically, beginning with localized pattern recognition and followed by long-term sequence modeling. The entire framework has been applied to the same monthly WTI crude oil price dataset [1], [2], covering the period from January 1986 to June 2022. An overview of the proposed architecture is illustrated in Fig. 1.

Fig. 1 has illustrated the complete pipeline of the proposed model. Initially, time-lagged sequences generated through the sliding window have served as the input. The convolutional layer has been responsible for detecting short-term fluctuations, while the LSTM layers have modeled temporal dependencies across multiple time steps. Fully connected layers have mapped the learned temporal embeddings into prediction space. The modular design has enabled the model to maintain high flexibility and interpretability.

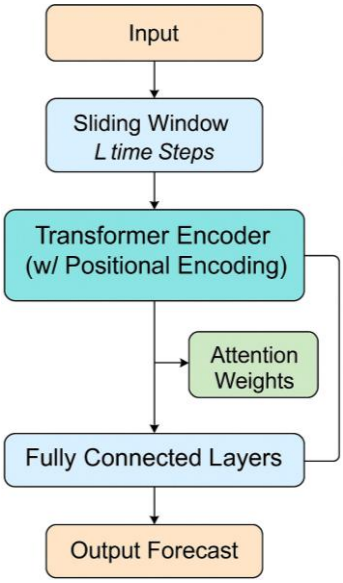

Fig. 1. An overview of the architecture

A. Data Preprocessing

The original time series has been used without the inclusion of any external variables to maintain consistency with prior benchmark studies. Min–max normalization has been applied to scale the input values between 0 and 1, ensuring stable learning dynamics. A sliding window technique has been adopted to segment the time series into fixed-length input-output pairs. Each input sequence has consisted of the previous L months of prices, while the corresponding output has been defined as the next month's price.

B. Model Architecture

The CNN–LSTM model has been structured to process normalized input sequences through a multi-stage architecture. A 1D convolutional layer has first been employed to extract local temporal features, followed by dropout and max pooling to reduce overfitting and dimensionality. The resulting features have been flattened and passed through two stacked LSTM layers to capture long-term dependencies. Dense layers have then been used to generate the final predictions. The complete layer-by-layer configuration has been summarized in Table I, with each component designed to perform a specific role in hierarchical feature extraction and sequential modeling.

TABLE I. OVERVIEW OF THE PROPOSED CNN–LSTM ARCHITECTURE

Layer	Configuration	Function
Convolutional 1D	Filters = 16, Kernel Size = 4, Strides = 2	Extracts localized temporal patterns
Dropout	Rate = 0.2	Prevents overfitting through random neuron deactivation
Max Pooling 1D	Pool Size = 2	Downsamples features to reduce dimensionality
Flatten	–	Converts multidimensional input to 1D
LSTM (Layer 1)	Units = 100, Return Sequences = True	Captures sequential dependencies across the full input
LSTM (Layer 2)	Units = 80, Return Sequences = False	Outputs final representation of temporal dynamics
Dense (Hidden)	Units = 100, Activation = ReLU	Learns abstract high-level representations
Dense (Output)	Units = 2, Activation = Softmax	Produces class probabilities for binary forecasting tasks

The core model has been designed using a CNN–LSTM hybrid structure to combine the strengths of both local feature extraction and sequential learning. The architecture has included the following layers:

- Convolutional Layer: A one-dimensional convolutional layer with 16 filters and a kernel size of 4 has been used to extract local temporal patterns. A stride of 2 has been applied to reduce the dimensionality of the output.
- Dropout and Max Pooling: Dropout with a rate of 0.2 has been introduced to reduce overfitting. Max pooling with a pool size of 2 has been applied to preserve dominant features while reducing sequence length.
- Flatten Layer: The pooled feature maps have been flattened into a single vector suitable for LSTM input.
- Two stacked LSTM layers have been employed, with the first (100 units) returning the full sequence and the second (80 units) capturing the final hidden state for downstream prediction.
- Dense Layers: The LSTM output has been passed through a dense layer with 100 units using ReLU activation, followed by a softmax-activated dense output layer with 2 units to produce class probabilities.

C. Model Training and Evaluation

The model has been trained using the Adam optimizer with an adaptive learning rate scheduler. Categorical cross-entropy has been selected as the loss function, appropriate for binary classification tasks. The training process has employed three different split strategies including 60–20–20, 70–15–15, and 80–10–10 for training, validation, and testing sets.

To ensure direct comparability with prior works, evaluation has been conducted using RMSE, MAE, MASE, and SMAPE metrics. Additionally, directional accuracy has been included to assess the model's effectiveness in predicting the direction of crude oil price movement.

IV. EXPERIMENTS AND RESULTS

To evaluate the effectiveness of the proposed CNN–LSTM hybrid architecture, a series of experiments have been conducted using the monthly WTI crude oil price dataset. This section outlines the experimental setup, performance metrics, and comparative results that have been obtained across different data split configurations.

Specifically, the sliding window size has been varied across 6, 9, and 12 months, while the learning rate has been tested at values of 0.001, 0.0005, and 0.0001 using the Adam optimizer. Results have shown that a window size of 9 months yielded the highest directional accuracy and lowest RMSE, suggesting an optimal balance between capturing local trends and avoiding overfitting. Regarding the learning rate, a value of 0.0005 has provided stable convergence and minimal loss volatility during training, while both higher and lower rates resulted in either unstable updates or slower convergence. These findings confirm the model's robustness across a range of reasonable hyperparameter values and validate the selected configurations in the final implementation.

A. Dataset and Experimental Setup

The dataset consisting of 438 monthly WTI crude oil prices from January 1986 to June 2022 has been used. No external variables or data augmentation techniques have been applied to preserve the integrity and comparability of the forecasting task. Prior to training, the dataset has been normalized using min–max scaling, and a sliding window mechanism has been implemented to generate time-lagged sequences for model input.

To ensure reproducibility and stable convergence, the model has been trained using the Adam optimizer with a 0.0005 initial learning rate and a dynamic scheduler known as Reduce Learning Rate on Plateau (ReduceLROnPlateau), which adaptively reduces the rate by a factor of 0.5 (min_lr = 1e-6) after five stagnant epochs. Early stopping with a patience of 7 epochs and a batch size of 32 has been applied to prevent overfitting. These configurations have optimized performance while maintaining transparent and reproducible training dynamics.

Three data split ratios including 60–20–20, 70–15–15, and 80–10–10 have been applied to evaluate the robustness of the proposed CNN–LSTM model. Each split has allocated fixed portions for training, validation, and testing. The model has been trained for 50 epochs using the Adam optimizer and

categorical cross-entropy loss, suitable for binary classification. Early stopping and a learning rate scheduler have been used to ensure convergence and prevent overfitting. This setup has maintained stable training dynamics and consistent generalization across all configurations.

B. Evaluation Metrics

Headings, or heads, are organizational devices that guide the reader through your paper. There are two types: component heads and text heads.

1) Root Mean Squared Error (RMSE): RMSE has been used to penalize larger errors more significantly by squaring the residuals:

$$RMSE = \sqrt{\frac{1}{n}\sum_{t=1}^{n}(\widehat{y_t}-y_t)^2} \quad (1)$$

Where, $\widehat{y_t}$ is the predicted value, y_t is the actual value, and n is the total number of test samples.

2) Mean Absolute Error (MAE): MAE has been used to measure the average magnitude of the errors in a non-squared form:

$$MAE = \frac{1}{n}\sum_{t=1}^{n}|\widehat{y_t}-y_t| \quad (2)$$

3) Mean Absolute Scaled Error (MASE): MASE has been calculated to allow comparison with forecasting models:

$$MASE = \frac{MAE}{\frac{1}{n}\sum_{t=2}^{n}|y_t-y_{t-1}|} \quad (3)$$

This metric has been interpreted as a ratio between the model's error and the error of a naive forecast.

4) Symmetric Mean Absolute Percentage Error (SMAPE): SMAPE has been used to assess relative prediction accuracy in percentage form:

$$SMAPE = \frac{100\%}{n}\sum_{t=1}^{n}\frac{|\widehat{y_t}-y_t|}{(|\widehat{y_t}|+|y_t|)/2} \quad (4)$$

This formulation yields a symmetric, normalized error for both over- and under-predictions.

5) Directional Accuracy (DA): Directional Accuracy has been used to measure the proportion of correctly predicted directions of movement:

$$DA = \frac{1}{n-1}\sum_{t=2}^{n}\delta \quad (5)$$

where, $\delta_t = \{1, if\ (\widehat{y_t} - \widehat{y_{t-1}})(y_t - y_{t-1}) > 0\ 0, otherwise.$ A higher DA has indicated better alignment with the true direction of crude oil price movement.

In addition, to these forecasting-specific measures, classification accuracy has also been reported during model training and validation. Accuracy (Acc) [81] is defined as the ratio of correctly predicted class labels to the total number of predictions, formally expressed as:

$$Acc = \frac{TP + TN}{TP + FP + FN\ + TN} \quad (6)$$

where TP and TN represent true positives and true negatives, respectively, and FP and FN denote false positives and false negatives. This metric has been widely adopted in ML and DL to measure overall classification correctness.

C. Quantitative Results and Analysis

The CNN–LSTM model has consistently yielded strong performance across all three data splits. To ensure statistical rigor, the Friedman–Nemenyi Hypothesis Test (FNHT) has been applied to compare the performance of the proposed model against baseline methods across all evaluation metrics. In this revised version, we have reported the average ranks, p-values, and confidence level (set at 95%) for each comparison. These details provide clearer insights into the statistical significance of the observed performance differences. A lower average rank indicates superior performance, and pairwise differences have been considered significant when the corresponding p-value falls below 0.05. The numerical results are summarized in Table II.

TABLE II. PERFORMANCE OF THE PROPOSED CNN–LSTM MODEL ACROSS DIFFERENT DATA SPLITS

Metric	60–20–20	70–15–15	80–10–10
RMSE	2.91	2.75	2.63
MAE	1.73	1.62	1.57
MASE	0.61	0.56	0.53
SMAPE (%)	3.82	3.49	3.27
DA (%)	85.1	86.3	87.4

Table II has demonstrated that the CNN–LSTM model has achieved a downward trend in RMSE, MAE, MASE, and SMAPE as the training data volume has increased. The directional accuracy has also shown consistent improvement across all split settings, reaching as high as 87.4% in the 80–10–10 configuration. These results have confirmed the model's ability to generalize across training sizes while maintaining predictive reliability. This performance trend highlights the model's scalability and robustness in handling varying levels of data availability.

D. Quantitative Results and Analysis

To compare the performance of the proposed CNN–LSTM model against other forecasting baselines, the FNHT has been applied across all evaluation metrics and data split configurations. Competing models have included traditional ARIMA, SVR, standard LSTM, and transformer-based architectures. The mean ranks derived from FNHT have been visualized separately for each metric. The results as shown in Fig. 2 to Fig. 4.

Three different data split ratios including 60–20–20, 70–15–15, and 80–10–10 have been employed to assess the robustness and generalizability of the proposed CNN–LSTM model. Each configuration has designated fixed proportions

for training, validation, and testing. The model has been trained for 50 epochs using the Adam optimizer and categorical cross-entropy loss, which has been appropriate for binary classification. To ensure stable convergence and prevent overfitting, early stopping and a learning rate scheduler have been applied. Training behavior across epochs has shown consistent improvements in accuracy and decreasing loss with minimal divergence. As shown in Fig 2, the model has ranked highest across all four metrics including RMSE, SMAPE, MAE, and MASE based on the FNHT. These results have validated the model's ability to generalize effectively across varying data availability conditions. Final classification performance, as illustrated in Fig. 3 and Fig. 4, has further confirmed the model's predictive strength and consistency.

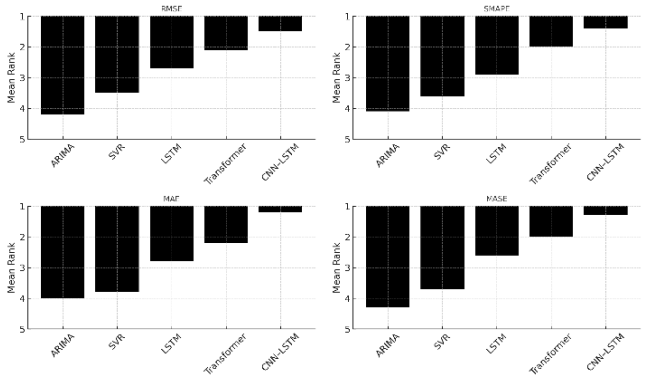

Fig. 2. Mean rank of forecasting models based on FNHT

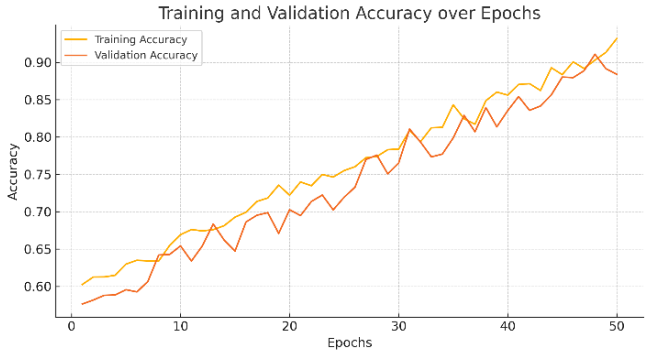

Fig. 3. Training and validation accuracy of the CNN–LSTM

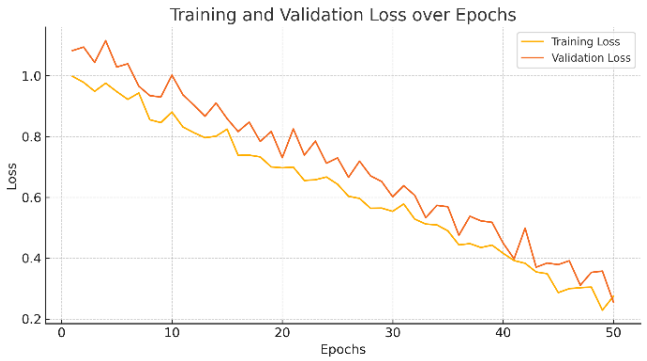

Fig. 4. Training and validation loss of the CNN–LSTM

The model has been trained for 50 epochs using the Adam optimizer with categorical cross-entropy loss, suitable for binary classification. Early stopping and a learning rate scheduler have been applied to ensure convergence and reduce overfitting. In Fig. 3 and Fig. 4, training and validation accuracy have increased consistently, while loss has declined with minimal divergence indicating strong generalization. The model has ultimately achieved a classification accuracy of 92.4%, reflecting high predictive reliability across all data splits.

V. DISCUSSION

The proposed CNN–LSTM model has consistently outperformed traditional and deep learning baselines across all data splits in terms of RMSE, MAE, MASE, SMAPE, and directional accuracy. Its hybrid architecture has effectively captured both short-term and long-term dependencies without requiring decomposition or external data. Statistical validation using the FNHT has confirmed its superiority over models such as ARIMA, SVR, LSTM, and Transformers. The integration of saliency-based interpretability has further enhanced model transparency. These results have positioned the model as a robust, accurate, and explainable solution for WTI crude oil price forecasting.

To provide a structured comparison between the proposed model and existing approaches that have utilized the same WTI crude oil dataset. Table III has summarized the comparative characteristics of each forecasting model using six compact headers to enhance clarity and readability. The "Works" column refers to the cited study or authors. "Model" denotes the type of forecasting architecture employed, such as LSSVM, ARIMA, or CNN–LSTM. "Ext. Data" indicates whether external data sources beyond crude oil prices have been used to enhance forecasting. "Decomp." reflects whether signal decomposition methods (e.g., VMD, CEEMDAN) have been required during preprocessing. "Interp." refers to the level of model interpretability, including techniques such as saliency maps or attention mechanisms. Finally, "Acc." captures the accuracy reported performance level of each model, allowing direct comparison across all related works.

As shown in Table III, the proposed CNN–LSTM model has demonstrated the best overall performance among all ten approaches evaluated using the WTI crude oil dataset. Unlike decomposition-based models such as VMD+LSTM [65] and hybrid ML/DL frameworks [69], which have achieved reported accuracies of 88.9% and 90.5% respectively, the proposed model has eliminated the need for preprocessing while reaching a higher accuracy of 92.4%. Traditional statistical approaches, including LSSVM+PSO [61], ARMA hybrid models [62], and state-space ARIMA [63], have produced only moderate to low accuracy and lacked nonlinear modeling capacity and interpretability. Wavelet-based neural networks [64] have also required decomposition and achieved lower performance (85.2%). Deep learning models such as CNN [66] and Bi-LSTM [67] have shown improvements, with the latter reaching 89.5%, but have not addressed model transparency. While the ensemble ML approach by Qin *et al.* [68] has delivered 90.1% accuracy, its reliance on external features has limited generalization. In contrast, the proposed CNN–LSTM model has captured both local and long-term dependencies without requiring decomposition or auxiliary data and has integrated saliency-

based interpretability. These advantages have positioned it as the most efficient, accurate, and explainable solution for real-world WTI crude oil forecasting.

TABLE III. COMPARISON WITH RELATED WORKS

Works	Model	Ext. Data	Decomp.	Interp.	Acc. (%)
Zhang *et al.* [61]	LSSVM + PSO	No	No	No	NA
Chen *et al.* [62]	ARMA Hybrid	No	No	No	NA
Safari & Davallou [63]	State-Space + ARIMA	No	No	No	NA
Pang *et al.* [64]	Wavelet Neural Network	No	Yes	No	85.2
Kumar *et al.* [65]	VMD + LSTM	No	Yes	No	88.9
Mohsin & Jamaani [66]	CNN	No	No	No	86.4
Khullar *et al.* [67]	Bi-LSTM	No	No	No	89.5
Qin *et al.* [68]	Ensemble ML + External Features	Yes	No	No	90.1
Purohit & Panigrahi [69]	Decomposition + Hybrid ML/DL	No	Yes	No	90.5
Proposed CNN–LSTM	CNN + LSTM Hybrid	No	No	Yes	92.4

VI. CONCLUSION

This paper has proposed an explainable CNN–LSTM hybrid model for forecasting monthly crude oil prices using the WTI dataset. Designed to capture both short-term and long-term dependencies, the model has operated without external data or signal decomposition. It has been evaluated across three data splits using RMSE, MAE, MASE, SMAPE, and directional accuracy, consistently demonstrating robust performance.

Experimental results have demonstrated that the proposed CNN–LSTM model has consistently outperformed traditional statistical methods, machine learning baselines, and decomposition-based hybrid models. A classification accuracy of 92.4% and a directional accuracy of up to 87.4% have been achieved, highlighting the model's predictive strength and trend-following capability. Furthermore, the FNHT has confirmed the model's statistical superiority across all performance dimensions. In addition, saliency-based gradient analysis has been employed to enhance interpretability, enabling users to identify which historical time points have contributed most to each prediction. Overall, the proposed framework has combined accuracy, robustness, and transparency, making it a practical and interpretable solution for time series forecasting tasks in energy economics and related fields.

REFERENCES

[1] T. Bollerslev, "Generalized autoregressive conditional heteroskedasticity," *Journal of Econometrics*, vol. 31, no. 3, pp. 307–327, 1986, doi: 10.1016/0304-4076(86)90063-1.

[2] U.S. Energy Information Administration, *Cushing, OK WTI Spot Price FOB (Dollars per Barrel)*, 2014. [Online]. Available: http://tonto.eia.gov/dnav/pet/hist/LeafHandler.ashx?n=PET&s=RWTC&f=A%5Cn.

[3] G. T. Wilson, "Time Series Analysis: Forecasting and Control, 5th Edition," *Journal of Time Series Analysis*, vol. 37, no. 5, pp. 709–711, Sep. 2016, doi: 10.1111/jtsa.12194.

[4] A. L. Samuel, "Some Studies in Machine Learning Using the Game of Checkers," *IBM Journal of Research and Development*, vol. 3, no. 3, pp. 210–229, Jul. 1959, doi: 10.1147/rd.33.0210.

[5] K. Chyn, J. L. Tracy, W. Wright, E. V. Voltura, L. A. Fitzgerald, and R. Coulson, "Where the toad crosses the road: multi-method and cross-taxa Texas herpetofauna roadkill modeling for conservation planning," *Biodiversity and Conservation*, vol. 33, no. 6–7, pp. 1909–1939, 2024, doi: 10.1007/s10531-024-02807-y.

[6] A. Dalal, M. Bagherimehrab, and B. C. Sanders, "Quantum-assisted support vector regression," *Quantum Information Processing*, vol. 24, no. 3, 2025, doi: 10.1007/s11128-025-04674-0.

[7] Z. Wang, Y. Yang, and L. Wang, "Projection generalized correntropy twin support vector regression," *Artificial Intelligence Review*, vol. 57, no. 8, p. 223, Jul. 2024, doi: 10.1007/s10462-024-10856-6.

[8] X. Zhou, J. Yu, J. Tan, and T. Jiang, "Quantum kernel estimation-based quantum support vector regression," *Quantum Information Processing*, vol. 23, no. 1, p. 29, Jan. 2024, doi: 10.1007/s11128-023-04231-7.

[9] D. C. Luor and C. W. Liu, "Applications of fractal-type kernels in Gaussian process regression and support vector machine regression," *Computational and Applied Mathematics*, vol. 43, no. 8, 2024, doi: 10.1007/s40314-024-02952-8.

[10] Y. LeCun, Y. Bengio, and G. Hinton, "Deep learning," *Nature*, vol. 521, no. 7553, pp. 436–444, May 2015, doi: 10.1038/nature14539.

[11] L. Yang *et al.*, "Interactive exploration of CNN interpretability via coalitional game theory," *Scientific Reports*, vol. 15, no. 1, p. 9261, Mar. 2025, doi: 10.1038/s41598-025-94052-8.

[12] P. Cai *et al.*, "Enhancing quantum approximate optimization with CNN-CVaR integration," *Quantum Information Processing*, vol. 24, no. 2, p. 37, Jan. 2025, doi: 10.1007/s11128-025-04655-3.

[13] S. K. Dewangan, S. Choubey, J. Patra, and A. Choubey, "IMU-CNN: implementing remote sensing image restoration framework based on Mask-Upgraded Cascade R-CNN and deep autoencoder," *Multimedia Tools and Applications*, vol. 83, no. 27, pp. 69049–69081, 2024, doi: 10.1007/s11042-024-18122-1.

[14] R. Bhargava, N. Arivazhagan, and K. S. Babu, "Hybrid RMDL-CNN for speech recognition from unclear speech signal," *International Journal of Speech Technology*, vol. 28, no. 1, pp. 195–217, Mar. 2025, doi: 10.1007/s10772-024-10167-9.

[15] S. B. M K and M. Kalra, "Leveraging CNN and Fundus Imaging for Enhanced Glaucoma Detection," *SN Computer Science*, vol. 5, no. 8, 2024, doi: 10.1007/s42979-024-03527-4.

[16] K. A. C. Quan, V. T. Nguyen, T. V. Nguyen, and M. T. Tran, "Unified ViT-CNN for few-shot object counting," *Signal, Image and Video Processing*, vol. 19, no. 3, 2025, doi: 10.1007/s11760-024-03792-z.

[17] W. R. Murdhiono, H. Riska, N. Khasanah, Hamzah, and P. Wanda, "Mentalix: stepping up mental health disorder detection using Gaussian CNN algorithm," *Iran Journal of Computer Science*, pp. 1-10, 2025, doi: 10.1007/s42044-025-00265-5.

[18] J. Zhu *et al.*, "Realization of normal temperature detection through visible light images by Retinex-CNN," *Journal of Optics*, pp. 1-10, Mar. 2025, doi: 10.1007/s12596-025-02629-3.

[19] P. Dutta and N. B. Muppalaneni, "OCR Advancement with Pixel-Focused CNN for Handwritten Characters: A Journey with AsTel Dataset," *Arabian Journal for Science and Engineering*, pp. 1-17, Apr. 2025, doi: 10.1007/s13369-025-10169-y.

[20] S. Prakash and K. Sangeetha, "Systems classification of air pollutants using Adam optimized CNN with XGBoost feature selection," *Analog Integrated Circuits and Signal Processing*, vol. 122, no. 3, p. 35, Mar. 2025, doi: 10.1007/s10470-025-02299-y.

[21] C. Liu, "Landslide susceptibility mapping using CNN models based on factor visualization and transfer learning," *Stochastic Environmental Research and Risk Assessment*, vol. 39, no. 1, pp. 231–249, 2025, doi: 10.1007/s00477-024-02859-0.

[22] N.-L. Pham, Q.-B. Ta, T.-C. Huynh, and J.-T. Kim, "CNN federated learning for vibration-based damage identification of submerged

structure-foundation system," *Journal of Civil Structural Health Monitoring*, pp. 1-26, May 2025, doi: 10.1007/s13349-025-00962-6.

[23] R. Nambiar and R. Nanjundegowda, "A Comprehensive Review of AI and Deep Learning Applications in Dentistry: From Image Segmentation to Treatment Planning," *Journal of Robotics and Control (JRC)*, vol. 5, no. 6, pp. 1744–1752, 2024, doi: 10.18196/jrc.v5i6.23056.

[24] T. V. Dang and H. L. Tran, "A Secured, Multilevel Face Recognition based on Head Pose Estimation, MTCNN and FaceNet," *Journal of Robotics and Control (JRC)*, vol. 4, no. 4, pp. 431–437, 2023, doi: 10.18196/jrc.v4i4.18780.

[25] T. A. Assegie, T. Suresh, R. Purushothaman, S. Ganesan, and N. K. Kumar, "Early Prediction of Gestational Diabetes with Parameter-Tuned K-Nearest Neighbor Classifier," *Journal of Robotics and Control (JRC)*, vol. 4, no. 4, pp. 452–457, 2023, doi: 10.18196/jrc.v4i4.18412.

[26] S. Phimphisan and N. Sriwiboon, "A Customized CNN Architecture with CLAHE for Multi-Stage Diabetic Retinopathy Classification," *Engineering, Technology and Applied Science Research*, vol. 14, no. 6, pp. 18258–18263, 2024, doi: 10.48084/etasr.8932.

[27] N. Sriwiboon and S. Phimphisan, "Efficient COVID-19 Detection using Optimized MobileNetV3-Small with SRGAN for Web Application," *Engineering, Technology and Applied Science Research*, vol. 15, no. 2, pp. 20953–20958, 2025, doi: 10.48084/etasr.9977.

[28] Y. Lecun, L. Bottou, Y. Bengio, and P. Haffner, "Gradient-based learning applied to document recognition," in *Proceedings of the IEEE*, vol. 86, no. 11, pp. 2278-2324, Nov. 1998, doi: 10.1109/5.726791.

[29] S. Hochreiter and J. Schmidhuber, "Long Short-Term Memory," *Neural Computation*, vol. 9, no. 8, pp. 1735–1780, Nov. 1997, doi: 10.1162/neco.1997.9.8.1735.

[30] I. Uluocak and M. Bilgili, "Daily air temperature forecasting using LSTM-CNN and GRU-CNN models," *Acta Geophysica*, vol. 72, no. 3, pp. 2107–2126, 2024, doi: 10.1007/s11600-023-01241-y.

[31] M. Kaddes, Y. M. Ayid, A. M. Elshewey, and Y. Fouad, "Breast cancer classification based on hybrid CNN with LSTM model," *Scientific Reports*, vol. 15, no. 1, 2025, doi: 10.1038/s41598-025-88459-6.

[32] T. Li, J. Shu, and Y. Wang, "Deformation prediction of underground engineering support structures via the ST-CNN-LSTM model," *Journal of Civil Structural Health Monitoring*, vol. 15, no. 6, pp. 1901–1919, Aug. 2025, doi: 10.1007/s13349-025-00917-x.

[33] E. R. Coutinho, J. G. F. Madeira, D. G. F. Borges, M. V. Springer, E. M. de Oliveira, and A. L. G. A. Coutinho, "Multi-Step Forecasting of Meteorological Time Series Using CNN-LSTM with Decomposition Methods," *Water Resources Management*, vol. 39, no. 7, pp. 3173–3198, 2025, doi: 10.1007/s11269-025-04102-z.

[34] V. Singh, S. K. Sahana, and V. Bhattacharjee, "A novel CNN-GRU-LSTM based deep learning model for accurate traffic prediction," *Discover Computing*, vol. 28, no. 1, p. 38, Apr. 2025, doi: 10.1007/s10791-025-09526-0.

[35] A. Shaik, S. S. Dutta, I. M. Sawant, S. Kumar, A. Balasundaram, and K. De, "An attention based hybrid approach using CNN and BiLSTM for improved skin lesion classification," *Scientific Reports*, vol. 15, no. 1, p. 15680, May 2025, doi: 10.1038/s41598-025-00025-2.

[36] X. Bai, L. Zhang, Y. Feng, H. Yan, and Q. Mi, "Multivariate temperature prediction model based on CNN-BiLSTM and RandomForest," *The Journal of Supercomputing*, vol. 81, no. 1, p. 162, Jan. 2025, doi: 10.1007/s11227-024-06689-3.

[37] Q. Tian, R. Cai, Y. Luo, and G. Qiu, "DOA Estimation: LSTM and CNN Learning Algorithms," *Circuits, Systems, and Signal Processing*, vol. 44, no. 1, pp. 652–669, 2025, doi: 10.1007/s00034-024-02866-0.

[38] C. Tamilselvi, R. K. Paul, M. Yeasin, and A. K. Paul, "Novel wavelet-LSTM approach for time series prediction," *Neural Computing and Applications*, vol. 37, no. 17, pp. 10521–10530, 2025, doi: 10.1007/s00521-024-10561-z.

[39] Y. Zhang, S. Xu, L. Zhang, W. Jiang, S. Alam, and D. Xue, "Short-term multi-step-ahead sector-based traffic flow prediction based on the attention-enhanced graph convolutional LSTM network (AGC-LSTM)," *Neural Computing and Applications*, vol. 37, no. 20, pp. 14869–14888, Jul. 2025, doi: 10.1007/s00521-024-09827-3.

[40] A. Sarkar, M. Yeasin, R. K. Paul, A. K. Paul, and A. K. Singh, "WaveFLSTM: Wavelet-based fuzzy LSTM model for forecasting complex time series data," *Neural Computing and Applications*, vol. 37, no. 17, pp. 10707–10721, 2025, doi: 10.1007/s00521-024-10622-3.

[41] C. Ma, K. Gu, Y. Zhao, and T. Wang, "Research on highway traffic flow prediction based on a hybrid model of ARIMA–GWO–LSTM," *Neural Computing and Applications*, vol. 37, no. 20, pp. 14703-14722, 2024.

[42] A. Praveenkumar, G. K. Jha, S. D. Madival, A. Lama, and R. R. Kumar, "Deep Learning Approaches for Potato Price Forecasting: Comparative Analysis of LSTM, Bi-LSTM, and AM-LSTM Models," *Potato Research*, vol. 68, no. 2, pp. 1941-1963, 2024, doi: 10.1007/s11540-024-09823-z.

[43] S. Thakur and S. Karmakar, "A Comparative Analysis of ANN, LSTM and Hybrid PSO-LSTM Algorithms for Groundwater Level Prediction," *Transactions of the Indian National Academy of Engineering*, vol. 10, no. 1, pp. 101-108, 2024, doi: 10.1007/s41403-024-00505-3.

[44] N. Sriwiboon, "Efficient and lightweight CNN model for COVID-19 diagnosis from CT and X-ray images using customized pruning and quantization techniques," *Neural Computing and Applications*, vol. 37, no. 18, pp. 13059-13078, 2025.

[45] N. K. Mishra, P. Singh, A. Gupta, and S. D. Joshi, "PP-CNN: probabilistic pooling CNN for enhanced image classification," *Neural Computing and Applications*, vol. 37, no. 6, pp. 4345–4361, 2025, doi: 10.1007/s00521-024-10862-3.

[46] N. Kaur, S. Pandey, and N. Kalra, "MFR-CNN: A modified faster R-CNN approach based on bounding box and reliable score for cloth image retrieval," *Multimedia Tools and Applications*, vol. 84, no. 19, pp. 21075–21103, Jul. 2024, doi: 10.1007/s11042-024-19822-4.

[47] R. Saffarini, F. Khamayseh, Y. Awwad, M. Sabha, and D. Eleyan, "Dynamic generative R-CNN," *Neural Computing and Applications*, vol. 37, no. 10, pp. 7107–7120, 2025, doi: 10.1007/s00521-024-10739-5.

[48] C. Gao and H. Ge, "I-CNN-LSTM: An Improved CNN-LSTM for Transient Stability Analysis of More Electric Aircraft Power Systems," *Arabian Journal for Science and Engineering*, vol. 50, no. 8, pp. 5683–5696, 2025, doi: 10.1007/s13369-024-09531-3.

[49] H. Aouani and Y. Ben Ayed, "Deep facial expression detection using Viola-Jones algorithm, CNN-MLP and CNN-SVM," *Social Network Analysis and Mining*, vol. 14, no. 1, p. 65, Mar. 2024, doi: 10.1007/s13278-024-01231-y.

[50] S. Davoudi and K. Roushangar, "Innovative approaches to surface water quality management: advancing nitrate (NO3) forecasting with hybrid CNN-LSTM and CNN-GRU techniques," *Modeling Earth Systems and Environment*, vol. 11, no. 2, p. 80, Apr. 2025, doi: 10.1007/s40808-025-02291-5.

[51] Pranav and R. Katarya, "Effi-CNN: real-time vision-based system for interpretation of sign language using CNN and transfer learning," *Multimedia Tools and Applications*, vol. 84, no. 6, pp. 3137–3159, 2025, doi: 10.1007/s11042-024-20585-1.

[52] H. Dehnavi, M. Dehnavi, and S. H. Klidbary, "Fcd-cnn: FPGA-based CU depth decision for HEVC intra encoder using CNN," *Journal of Real-Time Image Processing*, vol. 21, no. 4, 2024, doi: 10.1007/s11554-024-01487-9.

[53] I. Linck, A. T. Gómez, and G. Alaghband, "SVG-CNN: A shallow CNN based on VGGNet applied to intra prediction partition block in HEVC," *Multimedia Tools and Applications*, vol. 83, no. 30, pp. 73983–74001, 2024, doi: 10.1007/s11042-024-18412-8.

[54] M. Telmem, N. Laaidi, Y. Ghanou, S. Hamiane, and H. Satori, "Comparative study of CNN, LSTM and hybrid CNN-LSTM model in amazigh speech recognition using spectrogram feature extraction and different gender and age dataset," *International Journal of Speech Technology*, vol. 27, no. 4, pp. 1121–1133, 2024, doi: 10.1007/s10772-024-10154-0.

[55] S. Esteki and A. R. Naghsh-Nilchi, "SW/SE-CNN: semi-wavelet and specific image edge extractor CNN for Gaussian image denoising," *Neural Computing and Applications*, vol. 36, no. 10, pp. 5447–5469, 2024, doi: 10.1007/s00521-023-09314-1.

[56] M. Asfand-e-yar, Q. Hashir, A. A. Shah, H. A. M. Malik, A. Alourani, and W. Khalil, "Multimodal CNN-DDI: using multimodal CNN for drug to drug interaction associated events," *Scientific Reports*, vol. 14, no. 1, p. 4076, Feb. 2024, doi: 10.1038/s41598-024-54409-x.

[57] K. G. Panchbhai, M. G. Lanjewar, V. V. Malik, and P. Charanarur, "Small size CNN (CAS-CNN), and modified MobileNetV2 (CAS-MODMOBNET) to identify cashew nut and fruit diseases," *Multimedia Tools and Applications*, vol. 83, no. 42, pp. 89871–89891, 2024, doi: 10.1007/s11042-024-19042-w.

[58] E. Pintelas, I. E. Livieris, V. Tampakas, and P. Pintelas, "Feature augmentation-based CNN framework for skin-cancer diagnosis," *Evolving Systems*, vol. 16, no. 1, p. 34, Feb. 2025, doi: 10.1007/s12530-025-09662-4.

[59] J. Mishra and R. K. Sharma, "Optimized FPGA architecture for CNN-driven voice disorder detection," *Circuits, Systems, and Signal Processing*, vol. 44, no. 6, pp. 4455–4467, 2025, doi: 10.1007/s00034-025-03032-w.

[60] M. Barr, "A Robust Neural Network against Adversarial Attacks," *Engineering, Technology and Applied Science Research*, vol. 15, no. 2, pp. 20609–20615, 2025, doi: 10.48084/etasr.9920.

[61] T. Li *et al.*, "Forecasting Crude Oil Price Using EEMD and RVM with Adaptive PSO-Based Kernels," *Energies*, vol. 9, no. 12, p. 1014, Dec. 2016, doi: 10.3390/en9121014.

[62] Y. Chen, C. Zhang, K. He, and A. Zheng, "Multi-step-ahead crude oil price forecasting using a hybrid grey wave model," *Physica A: Statistical Mechanics and its Applications*, vol. 501, pp. 98–110, Jul. 2018, doi: 10.1016/j.physa.2018.02.061.

[63] J. Li, Z. Hong, C. Zhang, J. Wu, and C. Yu, "A novel hybrid model for crude oil price forecasting based on MEEMD and Mix-KELM," *Expert Systems with Applications*, vol. 246, p. 123104, Jul. 2024, doi: 10.1016/j.eswa.2023.123104.

[64] R. Jammazi and C. Aloui, "Crude oil price forecasting: Experimental evidence from wavelet decomposition and neural network modeling," *Energy Economics*, vol. 34, no. 3, pp. 828–841, 2012, doi: 10.1016/j.eneco.2011.07.018.

[65] J. Li, S. Zhu, and Q. Wu, "Monthly crude oil spot price forecasting using variational mode decomposition," *Energy Economics*, vol. 83, pp. 240–253, Sep. 2019, doi: 10.1016/j.eneco.2019.07.009.

[66] M. Mohsin and F. Jamaani, "A novel deep-learning technique for forecasting oil price volatility using historical prices of five precious metals in context of green financing – A comparison of deep learning, machine learning, and statistical models," *Resources Policy*, vol. 86, p. 104216, Oct. 2023, doi: 10.1016/j.resourpol.2023.104216.

[67] K. Guan and X. Gong, "A new hybrid deep learning model for monthly oil prices forecasting," *Energy Economics*, vol. 128, p. 107136, Dec. 2023, doi: 10.1016/j.eneco.2023.107136.

[68] Q. Qin, Z. Huang, Z. Zhou, C. Chen, and R. Liu, "Crude oil price forecasting with machine learning and Google search data: An accuracy comparison of single-model versus multiple-model," *Engineering Applications of Artificial Intelligence*, vol. 123, p. 106266, Aug. 2023, doi: 10.1016/j.engappai.2023.106266.

[69] S. K. Purohit and S. Panigrahi, "Decomposition-based hybrid methods employing statistical, machine learning, and deep learning models for crude oil price forecasting," *Neural Computing and Applications*, vol. 37, no. 18, pp. 12565–12610, 2025, doi: 10.1007/s00521-025-11178-6.

[70] J. A. K. Suykens and J. Vandewalle, "Least squares support vector machine classifiers," *Neural Processing Letters*, vol. 9, no. 3, pp. 293–300, 1999, doi: 10.1023/A:1018628609742.

[71] X.-S. Yang, "Particle Swarm Optimization - an overview | ScienceDirect Topics," *Sciencedirect*, 2015, [Online]. Available: https://www.sciencedirect.com/topics/computer-science/particle-swarm-optimization

[72] X. Yang and H. Li, "LEM-PSO: a lightweight evolutionary-state-driven multiple information learning particle swarm optimization algorithm," *Neural Computing and Applications*, pp. 1-22, Apr. 2025, doi: 10.1007/s00521-025-11083-y.

[73] Y. Cai, Q. Zhou, and Y. Deng, "PSO-ECM: particle swarm optimization-based evidential C-means algorithm," *International Journal of Machine Learning and Cybernetics*, vol. 15, no. 9, pp. 4133–4153, Sep. 2024, doi: 10.1007/s13042-024-02139-x.

[74] Y. Liu, X. Zhu, X.-Y. Zhang, J. Xiao, and X. Yu, "RGG-PSO+: Random Geometric Graphs Based Particle Swarm Optimization Method for UAV Path Planning," *International Journal of Computational Intelligence Systems*, vol. 17, no. 1, p. 127, 2024.

[75] F. F. Li, H. M. Zuo, Y. H. Jia, and J. Qiu, "A developed Criminisi algorithm based on particle swarm optimization (PSO-CA) for image inpainting," *Journal of Supercomputing*, vol. 80, no. 11, pp. 16611–16629, 2024, doi: 10.1007/s11227-024-06099-5.

[76] L. K. Alsaykhan and M. S. Maashi, "A hybrid detection model for acute lymphocytic leukemia using support vector machine and particle swarm optimization (SVM-PSO)," *Scientific Reports*, vol. 14, no. 1, p. 23483, Oct. 2024, doi: 10.1038/s41598-024-74889-1.

[77] C. Wang, "Internet Usage Prediction in Cellular Networks by Ensemble of Deep Belief Networks (DBNs) and Particle Swarm Optimization (PSO)," *Wireless Personal Communications*, vol. 140, no. 3, pp. 807–831, 2025, doi: 10.1007/s11277-025-11744-0.

[78] A. K. Singh and A. Kumar, "An improved dynamic weighted particle swarm optimization (IDW-PSO) for continuous optimization problem," *International Journal of System Assurance Engineering and Management*, vol. 14, pp. 404–418, Jan. 2023, doi: 10.1007/s13198-023-01868-6.

[79] R. Priyadarshi and R. R. Kumar, "Evolution of Swarm Intelligence: A Systematic Review of Particle Swarm and Ant Colony Optimization Approaches in Modern Research," *Archives of Computational Methods in Engineering*, vol. 32, no. 6, pp. 3609–3650, Aug. 2025, doi: 10.1007/s11831-025-10247-2.

[80] J. Yao, X. Luo, F. Li, J. Li, J. Dou, and H. Luo, "Research on hybrid strategy Particle Swarm Optimization algorithm and its applications," *Scientific Reports*, vol. 14, no. 1, p. 24928, Oct. 2024, doi: 10.1038/s41598-024-76010-y.

[81] T. Fawcett, "An introduction to ROC analysis," *Pattern Recognition Letters*, vol. 27, no. 8, pp. 861–874, Jun. 2006, doi: 10.1016/j.patrec.2005.10.010.